Development 136, 3433-3442 (2009) doi:10.1242/dev.037226

Lineage-specific cell death in postembryonic brain development of *Drosophila*

Abhilasha Kumar, Bruno Bello and Heinrich Reichert*

The *Drosophila* central brain is composed of thousands of neurons that derive from approximately 100 neuroblasts per hemisphere. Functional circuits in the brain require precise neuronal wiring and tight control of neuronal numbers. How this accurate control of neuronal numbers is achieved during neural development is largely unclear. Specifically, the role of programmed cell death in control of cell numbers has not been studied in the central brain neuroblast lineages. Here, we focus on four postembryonic neuroblast lineages in the central brain identified on the basis that they express the homeobox gene *engrailed* (*en*). For each lineage, we determine the total number of adult-specific neurons generated as well as number and pattern of *en*-expressing cells. We then demonstrate that programmed cell death has a pronounced effect on the number of cells in the four lineages; approximately half of the immature adult-specific neurons in three of the four lineages are eliminated by cell death during postembryonic development. Moreover, we show that programmed cell death selectively affects *en*-positive versus *en*-negative cells in a lineage-specific manner and, thus, controls the relative number of *en*-expressing neurons in each lineage. Furthermore, we provide evidence that Notch signaling is involved in the regulation of *en* expression. Based on our findings, we conclude that lineage-specific programmed cell death plays a prominent role in the generation of neuronal number and lineage diversity in the *Drosophila* brain.

KEY WORDS: *Drosophila*, Brain, *engrailed*, Cell death, Lineage, Neuroblast, Stem cell, Notch

INTRODUCTION

The *Drosophila* brain is generated by approximately 100 neural-stem-cell-like neuroblasts that derive from the cephalic neuroectoderm in the early embryo (Urbach and Technau, 2003b). In the embryo, neuroblasts divide repeatedly in an asymmetric mode, whereby they self-renew and generate an intermediate progenitor cell called a ganglion mother cell (GMC). The GMC usually divides once to produce two postmitotic progeny (Knoblich, 2008; Pearson and Doe, 2004; Skeath and Thor, 2003). Following a brief period of quiescence, during postembryonic larval development, neuroblasts re-enter the cell cycle and continue to divide in this asymmetric mode, giving rise to adult-specific neurons, which make up more than 90% of the adult central nervous system (CNS) (Prokop and Technau, 1991; Truman and Bate, 1988). The adult-specific neurons generated during larval life from each neuroblast form a lineage-related cluster of immature neurons, which wait until metamorphosis to differentiate and form functional circuits in the adult (Dumstrei et al., 2003; Pereanu and Hartenstein, 2006; Truman et al., 2004; Zheng et al., 2006).

It is generally believed that each postembryonic neuroblast generates between 100 to 150 neurons [for exceptions, see Bello et al. (Bello et al., 2008), Boone and Doe (Boone and Doe, 2008) and Bowman et al. (Bowman et al., 2008)]. It is thought that an autonomous program in the neuroblast determines its proliferative capacity, and thereby number of cells that constitute its lineage (reviewed by Hidalgo and Constant, 2003). Studies addressing this issue have pointed to two possible mechanisms: regulation of neuroblast proliferation and elimination of a precursor neuroblast or its progeny, the postmitotic neurons, through programmed cell death.

Biozentrum, University of Basel, Klingelbergstrasse 50, CH-4056 Basel, Switzerland.

*Author for correspondence (heinrich.reichert@unibas.ch)

Accepted 14 August 2009

Programmed cell death has been reported to occur widely in the fly CNS. In the late embryo, prominent cell death appears throughout the CNS as the ventral nerve cord (VNC) condenses (Abrams et al., 1993). Among the cells in the VNC are neuroblasts of abdominal neuromeres that die via a *reaper*-dependent mechanism (Peterson et al., 2002). Moreover, recent systematic analysis of the number and identity of dying cells in the embryonic VNC implies that there might be a strict spatiotemporal regulation in cell-death pattern (Rogulja-Ortmann et al., 2007).

Studies conducted on identified neuroblast lineages have pointed to possible mechanisms involved in elimination of neuroblasts or postmitotic neuronal/glial cells. For instance, Hox genes are shown to be involved in regulation of programmed cell death in the developing CNS. In the embryonic VNC, *Abdominal B* (*Abd-B*) expression is essential for survival of differentiated neurons in the posterior segments (Miguel-Aliaga and Thor, 2004). In the larval VNC, neuroblasts of the abdominal segments undergo apoptosis following a pulse of *abdominal A* (*abd-A*) expression, thus regulating neuronal numbers (Bello et al., 2003). In addition, *Ultrabithorax* (*Ubx*) and *Antennapedia* (*Antp*) act antagonistically in differentiated motoneurons of the neuroblast 7-3 (NB7-3) and NB2-4t lineages to regulate apoptosis (Rogulja-Ortmann et al., 2008). The NB7-3 lineage in the embryonic VNC has been extensively studied, and identified neurons of this lineage have been shown to undergo cell death (Karcavich and Doe, 2005; Lundell et al., 2003; Novotny et al., 2002). Programmed cell death has also been reported for midline glial cells during embryonic life (Sonnenfeld and Jacobs, 1995) and during metamorphosis, when ecdysteroids play a key role in inducing cell death (Awad and Truman, 1997).

Although the intrinsic and extrinsic determinants controlling lineage- and neuron-specific programmed cell death in the developing CNS are poorly understood, there is some evidence that cell-fate determinants Notch and Numb are involved (Karcavich, 2005). During GMC division, the Numb protein is segregated asymmetrically from the GMC to one of its two sibling daughter

cells (reviewed by Cayouette and Raff, 2002; Lu et al., 2000; Skeath and Thor, 2003). In consequence, Numb blocks Notch signaling in this GMC daughter and allows the cell to assume a 'B-fate'. By contrast, in the other GMC daughter that does not receive Numb, Notch signaling occurs, and hence that cell assumes a different 'A-fate'. Importantly, as demonstrated for the lineage of NB7-3, this interaction between Numb and Notch can be responsible for controlling programmed cell death; the daughter cell of GMC-2, in which Numb inhibits Notch signaling, survives, whereas its sibling, in which Notch signaling is active, is programmed to die (reviewed by Karcavich, 2005). A similar binary cell death decision has been demonstrated in the lineage giving rise to multidendritic neuron vmd1a in the peripheral nervous system (Orgogozo et al., 2002). Broadly speaking, Notch/Numb signaling may be acting generically as an important mechanism, enabling the two siblings of each GMC to acquire different fates, and hence give rise to neuroblast lineages that comprise two sublineages ('B-hemilineage' and 'A-hemilineage'), each with different cell-fate potential.

Until now, most of the studies addressing the issue of cell death and differential cell fate have been done in the VNC. In contrast, very little is known about these processes in the central brain. In this study, we identify four postembryonic neuroblast lineages in the central brain based on the criterion that they express the homeobox gene, *en*. For each lineage, we show that they have a characteristic, relatively invariant lineage size as well as a lineage-specific number of *en*-expressing cells. We then demonstrate that programmed cell death dramatically influences number of cells in three of the four lineages. In these three, approximately half the neurons in each lineage are eliminated by programmed cell death. Furthermore, we show that programmed cell death specifically targets *en*-negative cells in two of the three lineages, whereas in the third lineage, *en*-positive cells are selected to die. In this manner, differential cell death controls the relative number of *en*-expressing neurons in each lineage. Finally, we provide evidence that Notch signaling is involved in regulation of *en* in each of the four lineages. In conclusion, our data indicate that lineage-specific programmed cell death plays a significant role in controlling neuronal number and in generating lineage diversity in the *Drosophila* brain.

MATERIALS AND METHODS

Fly strains and genetics

For mosaic analysis with a repressible cell marker (MARCM) experiments, embryos of appropriate genotype were collected on standard cornmeal/yeast medium over a 4-hour window and raised at 25°C for 21-25 hours (or 44-48 hours; see Fig. 6) before heat-shock treatment. (Before these 4 hours, flies were allowed to lay eggs for 2 hours on fresh yeast to synchronize egg laying.) Heat-shock induction of FLP was done at 37°C for 60 minutes. MARCM clones were examined in brains dissected at late third-instar larval stage (L3). Unless otherwise indicated, all stocks were obtained from Bloomington Stock Center, Indiana, USA.

To generate wild-type MARCM clones (Lee and Luo, 1999) females of driver stock y,w,hsFLP; FRT40A, tubPGAL80^{LL10}/CyO,ActGFP^{JMR1}; tubP-GAL4^{LL7}, UAS-mCD8::GFP^{LL6}/TM6,Tb,Hu were mated to w; FRT40A, UAS-mCD8::GFP^{LL5} males. Homozygous H99 MARCM clones were generated (Bello et al., 2003) by crossing females of driver stock y,w,hsFLP; tubP-Gal4, UAS-mCD8::GFP^{LL5}/CyO, ActGFP^{JMR1}; FRT2A, tubP-Gal80^{LL9}/TM6, Tb, Hu with w; FRT2A, H99, kni^{ri}-2/TM6[w^{+}] males. Homozygous Notch mutant MARCM clones were generated using a recombinant null allele FRT19A, N^{55e11}/FM7 KrGal4 UAS-GFP. Females were mated with males of driver stock FRT19A, tubP-Gal80^{LL1}, hsFLP, w*; tubP-Gal4, UAS-mCD8::GFP^{LL5}/CyO, ActGFP^{JMR1}. In these experiments, *notch* allele on the X chromosome was recombined with FRT 19A; in consequence, the resulting MARCM clones obtained using this FRT were low in frequency.

Immunolabeling

Late L3 brains were dissected in PBS, fixed and immunostained as previously described (Bello et al., 2007). The following antibodies were used: mouse anti-Engrailed 4D9 [1:10; Developmental Studies Hybridoma Bank (DSHB)], rabbit anti-GFP (1:450; Torrey Pines Biolabs) and rat anti-Elav Mab7E8A10 (1:30; DSHB). Secondary antibodies: Alexa Fluor 488, Alexa Fluor 568 and Alexa Fluor 647 generated in goat (1:300; Molecular Probes).

Microscopy and image processing

All fluorescent images were recorded using a Leica TCS SP scanning confocal microscope. Complete series of optical sections were taken at 1 μm intervals with picture size of 512 × 512 pixels. Digital image stacks were processed using ImageJ. To visualize *en*-expressing MARCM clones, image stacks with few non-interfering clones were selected, and stained processes as well as cell bodies from other clones were removed using the lasso tool in every single optical section. For cell counts, cells were marked per section in the selected confocal *z* stack and counted using the 'cell counter' plugin of ImageJ. Means for all histograms are indicated in the text. Error bars indicate s.d., values for which are indicated in the text. Sample sizes for all histograms are indicated in corresponding figure legends.

RESULTS

Four neuroblast lineages produce the *engrailed*-expressing neurons in the postembryonic central brain

The *en* gene is expressed in metamerically reiterated stripes in the embryonic neuroectoderm, in some neuroblasts (and GMCs) that derive from these neuroectodermal domains, and in well-defined groups of postmitotic primary and secondary neurons, usually located at the posterior boundary of each CNS neuromere (Bossing et al., 1996; Schmid et al., 1999; Urbach and Technau, 2003a; Urbach and Technau, 2003c; Younossi-Hartenstein et al., 1996). In our analysis of mechanisms involved in the control of neuronal cell number, we focused specifically on a set of *en*-expressing neural cells in the *Drosophila* central brain (supraesophageal ganglion without optic lobes).

Analysis of the adult central brain using anti-En immunocytochemistry indicated that characteristic numbers of *en*-expressing cells were present and arranged in fixed spatial patterns. In particular, three spatially separated clusters of *en*-positive cell bodies were manifest (Fig. 1A,B). We refer to these clusters as the anterior cluster (AC), medial cluster (MC) and posterior cluster (PC). (Numerous *en*-expressing cells were also seen in the subesophageal ganglion; these cells were not characterized further in this study.) Analysis of late L3 brain showed that the general arrangement of the *en*-expressing cell clusters in the supraesophageal ganglion was already established by the end of larval development (Fig. 1C).

The clustered arrangement of these *en*-positive cells suggests that they might belong to several neuroblast lineages. [In the lineages of the central brain, the neuroblast and the secondary postmitotic neurons generated by this neuroblast form a tight cluster at least until metamorphosis (see Dumstrei et al., 2003).] To investigate the lineage-dependent origin of *en*-expressing cells in more detail, we carried out a MARCM-based clonal analysis with a ubiquitous tubulin-Gal4 driving UAS-mCD8::GFP and selected labeled, secondary clones for analysis that contained immunolabeled *en*-positive cells. In this analysis, we consistently recovered neuroblast clones containing *en*-positive cells in the central brain that corresponded to four different neuroblast lineages (Fig. 1D-G). Whereas cells of the AC cluster belonged to one lineage and cells of the PC cluster belonged to another lineage, cells of the MC cluster belonged to two different lineages that were closely apposed in the brain. We refer to the two lineages that make up the MC cluster as MC1 and MC2 lineages. Based on location

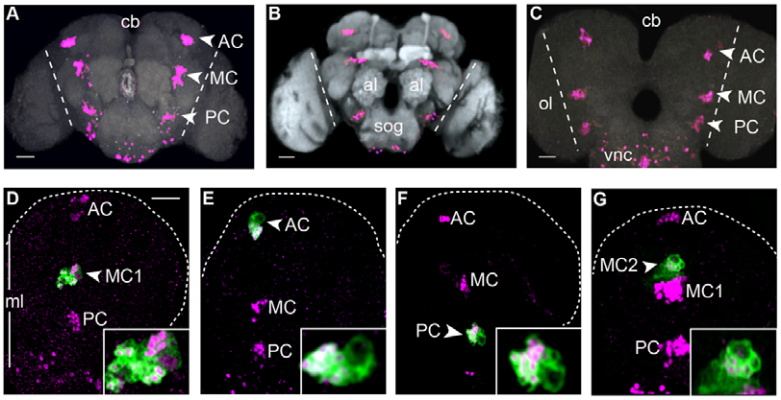

Fig. 1. *engrailed* is expressed in three clusters in the *Drosophila* postembryonic central brain. Anti-Engrailed (En) staining is in magenta. (**A**,**C**) Frontal view, maximal projections of wild-type (Oregon R) adult (A) and L3 (C) brain. Arrowheads, *en*-expressing clusters: anterior cluster (AC), medial cluster (MC) and posterior cluster (PC). (**B**) Frontal view, maximal projection of adult brain [*y,w; rbo*^{2}*; rbo-eGFP* (Huang et al., 2004)]. Anti-GFP (gray) highlights the neuropile. (**D-G**) Frontal view of L3 brains; the right hemisphere is shown (outlined). The three *en*-expressing clusters correspond to four neuroblast lineages in L3. *z*-projections of selected panels of wild-type GFP-labeled MARCM clones expressing *en* (inset shows higher magnification). (D) MC1, (E) AC, (F) PC and (G) MC2 lineage. Scale bars: 50 μm in A-C; 30 μm in D-G. al, antennal lobes; cb, central brain; ml, midline; ol, optic lobes; sog, subesophageal ganglion; vnc, ventral nerve cord.

of cell bodies, projection of secondary axon tracts, and the innervated set of compartments, we identified these four lineages, according to criteria and terminology established by Pereanu and Hartenstein (Pereanu and Hartenstein, 2006), as DPLam (AC), DALv2 (MC1), DALv3 (MC2) and BAla3 (PC); the AC, MC1 and MC2 lineages are thus protocerebral and the PC lineage is deutocerebral (Kumar et al., 2009).

Number and spatial pattern of *engrailed*-expressing neuronal cells are lineage specific

Although our clonal analysis indicated that the *en*-expressing cells in the central brain belong to four lineages, not all cells in these four lineages expressed *en*. The overall lineage size (all GFP-positive cells in a clone, excluding the neuroblast) and the number of *en*-positive cells (GMCs and differentiated neurons) were found to be different for the four lineages (Fig. 2). In terms of overall cell number, the MC1 lineage was strikingly larger than the other three lineages. MC1 neuroblast clones contained approximately 130 cells, whereas AC, PC and MC2 neuroblast clones comprised 60-80 cells. The MC1 neuroblast clones also had the largest number of *en*-expressing cells (an average of 87±7.2). The AC and PC neuroblast clones had somewhat fewer *en*-positive cells (averages of 63±5.9, for AC, 55±4.7 for PC) and, remarkably, the MC2 neuroblast clone had fewer than 20 (17±3.4) *en*-positive cells.

To characterize the lineage-specific differences in more detail, we combined MARCM-based clonal analysis with anti-En and neuron-specific marker labeling (anti-Elav) and analyzed the spatial arrangement of *en*-positive versus *en*-negative cells in all four lineages at late L3. In the MC1 lineage, the large cortically located neuroblast and an average of 10±3.1 immediately adjacent GMCs and undifferentiated neurons consistently expressed *en* (Fig. 2, Fig. 3A). In addition to the neuroblast and GMCs, the clone contained a large number of Elav-expressing cells that represent secondary neurons of the lineage. Approximately two-thirds of these neurons were *en*-positive and one-third were *en*-negative (Fig. 3A,A′; see Fig. 5A′). When labeled clones were examined at different levels that extended from the outer cortical layer towards the central neuropile, there was no obvious segregation into clonal subregions containing preferentially *en*-positive or *en*-negative neurons. Rather, both types of neurons appeared to be spatially intermixed throughout the MARCM clone (summarized in Fig. 3A″).

In the AC and PC lineages, the large neuroblast and the adjacent small group of GMC-like cells (averages of 15±3.8 and 9±1.8, respectively) did not express *en* (Fig. 2, Fig. 3B,C). In addition to the neuroblast and GMC-like cells, the clones contained a large number of Elav-expressing cells representing secondary neurons of the lineage. Almost all of these neurons were positive for *en*; only a very small number (<5) were negative for *en* (Fig. 3B,B′,C,C′, Fig. 5B,B′,C,C′). Thus, in both AC and PC lineages, virtually all the neurons throughout all clonal subregions extending from the outer cortical layer towards the central neuropile expressed *en* (summarized in Fig. 3B″,C″).

Finally, in the MC2 lineage, as in MC1, the neuroblast and the small group of (average 10±1.8) adjacent GMC-like cells expressed *en* (Fig. 2, Fig. 3D,D′). Expression of *en* was also observed in a small number of Elav-expressing secondary neurons (<10) located near the neuroblast. Based on their position relative to the neuroblast, these neurons may be recently born. However, the remaining secondary neurons in all clonal subregions of MC2 lineage were consistently negative for *en* (Fig. 3D,D′, Fig. 5D′). Thus, in contrast to their neuroblast of origin, most neurons in MC2 did not express *en* (summarized in Fig. 3D″).

In summary, we observed a striking neuronal heterogeneity among the lineages that contain *en*-expressing adult-specific neurons in the brain. The MC1 lineage is the largest in terms of its cell number

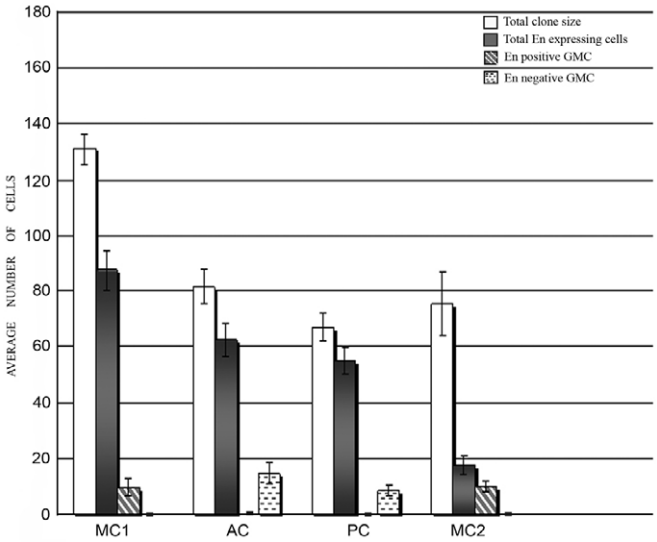

Fig. 2. Clone size difference between *engrailed*-expressing lineages. Bar chart showing total clone size (all GFP-positive cells, excluding neuroblast), the number of *en*-expressing cells (Elav-negative GMCs and Elav-positive neurons) and the number of *en*-positive and *en*-negative GMCs of the four wild-type MARCM clones. The average number of cells is plotted against the type of lineage. Sample size (*n*): MC1, AC, PC, *n*=12 each; MC2, *n*=7. Error bars indicate s.d.

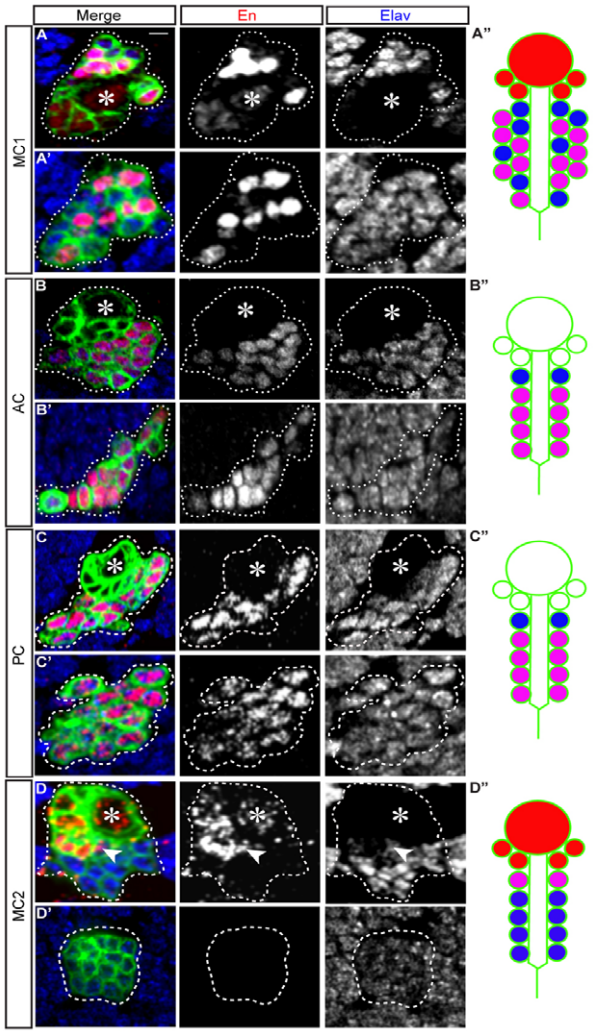

Fig. 3. Lineage-specific expression of *engrailed*. (**A-D″**) Single sections of wild-type MARCM clones stained with anti-GFP (green), anti-En (red) and anti-Elav (blue). White dotted lines outline clones. Asterisk indicates neuroblast. Lineages were as follows: MC1 (A,A′), AC (B,B′), PC (C,C′) and MC2 (D,D′). (A-D) Optical section at a superficial focal plane. (A,D) Neuroblast and newborn progeny express *en*. (D) The white arrowhead indicates an *en*-positive neuron. (A′-D′) Optical section at a deeper focal plane. (A″-D″) Schematics representing MC1, AC, PC and MC2, respectively. Color coding is according to immunostaining, i.e. schematic *en*-positive and -negative neurons are in pink and blue, respectively. Scale bar: 10 μm.

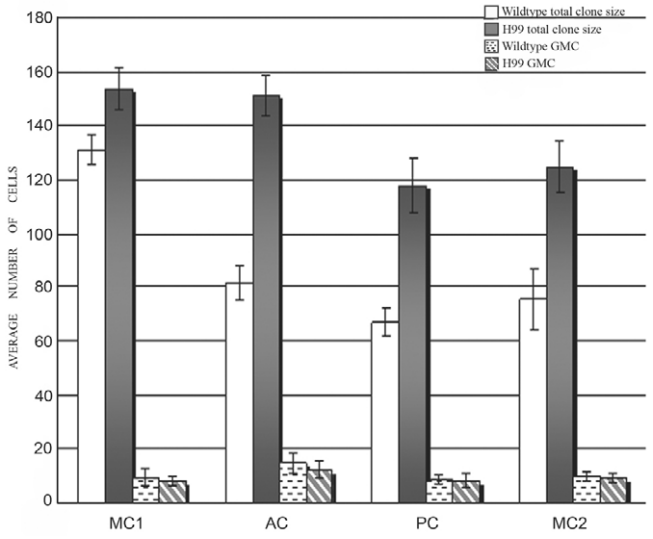

Fig. 4. Effect of blocking cell death on total clone size of *engrailed*-expressing lineages. Bar chart showing the difference in total clone size (all GFP-positive cells, excluding neuroblasts) and GMCs (all Elav-negative, but *en*-positive or *en*-negative cells) between wild-type and H99 *en* lineages. Sample size (*n*) for H99 lineages: MC1, AC, PC, *n*=12 each; MC2, *n*=9. Error bars indicate s.d.

compared with the other three, and the secondary neurons of MC1 are a mixture of both *en*-positive and *en*-negative cells. The AC and PC lineages are comparable in size and have a similar pattern of *en* expression; almost all the neurons in these two lineages express *en*. The MC2 lineage, although comparable in size to the AC and PC lineages, is drastically different in terms of its *en* expression in that almost all neurons in the MC2 lineage do not express *en*.

Programmed cell death shapes neuroblast lineage size in postembryonic brain development

To investigate if lineage-specific programmed cell death is involved in determining the total number of cells in these lineages, we blocked apoptosis by generating H99 mutant MARCM neuroblast clones in which the three pro-apoptosis genes *head involution defective* (*hid*; *Wrinkled* – FlyBase), *grim* and *reaper* (*rpr*) were eliminated in the genomic region at 75C, due to a homozygous deficiency Df3(3L)H99 (Chen et al., 1996; Grether et al., 1995; White et al., 1994). We then quantified the number of cells in wild type versus H99 clones for each *en* lineage. Both types of clones were co-immunolabeled with anti-En and anti-Elav. Due to lack of programmed cell death, the total number of cells in all four lineages increased, whereas the number of GMCs remained comparable to wild type (Fig. 4). However, the magnitude of these increases was markedly different for the MC1 lineage compared with the AC, PC and MC2 lineages.

In the H99 MC1 lineage, a relatively small increase in total cell number from an average of 131±5.5 cells to an average of 154±7.7 cells was observed. In contrast, in the H99 AC lineage, a striking increase from an average of 81±6.3 cells to an average of 151±7.6 cells was seen. This value, which corresponded to an approximate doubling in cell number in H99 AC lineages, was similar to the total number of cells observed in the H99 MC1 lineage. Comparable, albeit slightly less pronounced, increases were observed in the PC lineage (increase in average cell number from 67±5 to 118±10) and the MC2 lineage (increase in average cell number from 75±11.4 to 125±9.6) following apoptosis block. The marked increase in total cell number observed in H99 clones of AC, PC and MC2 lineages indicates that programmed cell death plays a major role in determining the size of these lineages, whereas it appears to have only a minor role in size control of the MC1 lineage.

Programmed cell death controls the number of *engrailed*-expressing neurons in a lineage-specific manner

Given the role of programmed cell death in determining the total cell number in wild type and H99 clones (Fig. 4), we wondered if cell death determines the number of neurons in a lineage-specific manner. To investigate this, we quantified the number of *en*-positive and *en*-negative neurons in wild type versus H99 MARCM clones for each lineage.

In the MC1 neuroblast clones, the number of *en*-positive neurons was similar in H99 and wild type; however, the number of *en*-negative neurons increased from approximately 44±6.3 in wild type to 71±6 in H99 clones (Fig. 5A,A′). This implies that the increase in overall cell number observed in H99 MC1 clones (Fig. 4) is due primarily to an increase in number of surviving *en*-negative neurons. This results in an approximately equal number of *en*-negative and *en*-positive secondary neurons in H99 MC1 clones (summarized in Fig. 5A″).

In H99 AC and PC neuroblast clones, the number of *en*-positive neurons was comparable to that in wild type. However, the number of *en*-negative neurons increased dramatically from 4±2.5 cells in wild type to 72±5.6 cells for AC clones and from 3±1.7 cells in wild type to 55±6.1 cells for PC clones following apoptosis block (Fig. 5B,B′,C,C′). Indeed, the marked increase in overall cell number observed in H99 AC and PC clones (Fig. 4) appears to be almost exclusively due to an increase in the number of surviving *en*-negative neurons. Thus, after apoptosis block, these neuroblast clones also contained approximately equal numbers of *en*-negative and *en*-positive secondary neurons (summarized in Fig. 5B″,C″).

In the MC2 neuroblast clones, the number of *en*-positive neurons was clearly affected by apoptosis block and increased markedly from 8±3.6 in wild type to approximately 39±9.8 cells in apoptosis-blocked clones (Fig. 5D,D′). By contrast, the number of *en*-negative neurons showed a much smaller increase in wild type versus H99 clones. Thus, in contrast to the other three lineages, the striking increase in cell number observed in H99 MC2 clones (Fig. 4) appears to be due primarily to an increase in number of surviving *en*-positive neurons (summarized in Fig. 5D″).

Taken together, these findings indicate that programmed cell death has lineage-specific effects on *en*-positive and *en*-negative neurons in the postembryonic brain. In the MC1 lineage, programmed cell death eliminates some *en*-negative neurons but does not affect *en*-positive neurons. In the AC and PC lineages, programmed cell death

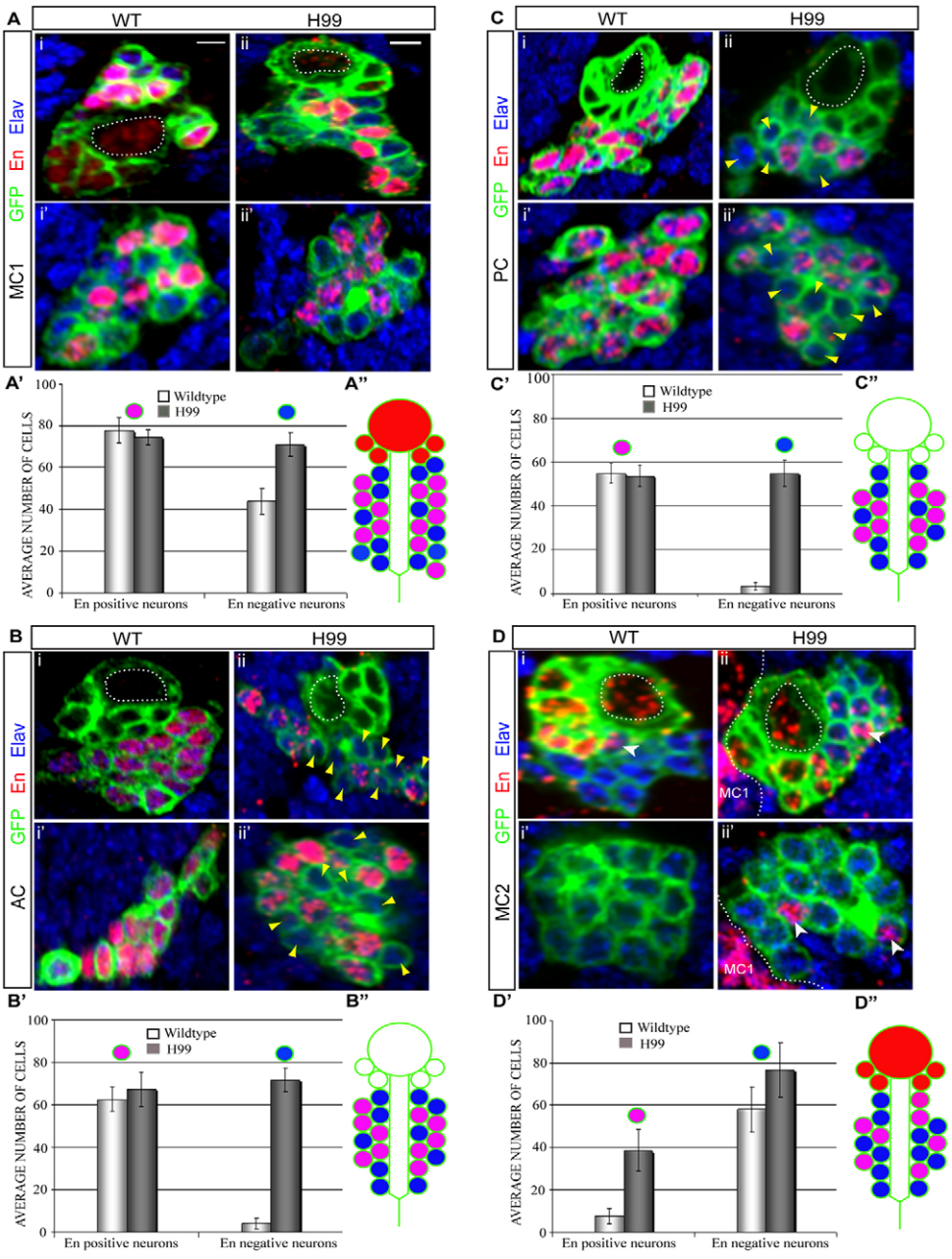

Fig. 5. Lineage-specific effect of blocking cell death on number of *engrailed*-expressing neurons. (**A-D**) *z*-projections of wild-type (i-i′) and H99 (ii-ii′) MARCM clones (MC1, AC, PC and MC2, respectively) stained with anti-GFP (green), anti-En (red) and anti-Elav (blue). White dotted lines outline neuroblasts. Top row (i,ii): superficial optical section. Bottom row (i′,ii′): deeper optical section. Yellow arrowheads indicate *en*-negative neurons; white arrowheads indicate *en*-positive neurons. (**A′-D′**) Bar charts showing effect of blocking cell death (H99) on the number of *en*-positive and *en*-negative neurons, as compared with wild type. White and gray bars indicate wild-type and H99 *en*-lineages, respectively. The left-hand bars indicate the number of *en*-positive neurons, whereas the right-hand bars indicate the number of *en*-negative neurons. (**A″-D″**) Schematics of H99 MC1, AC, PC and MC2 MARCM clones, respectively. Color coding is according to immunostaining. Error bars indicate s.d. Scale bars: 10 μm.

eliminates virtually all *en*-negative neurons, but does not affect *en*-positive neurons. By contrast, in the MC2 lineage, programmed cell death eliminates the majority (approximately three-quarters) of the *en*-positive neurons but affects only few *en*-negative neurons.

Evidence for a hemilineage-specific effect of programmed cell death on *engrailed* expression

The observed lineage-specific effects of programmed cell death on neuronal number and *en* expression support a model in which each of the four neuroblasts generates two distinct hemilineages. In this model, each GMC division gives rise to one *en*-positive and one *en*-negative neuron, which are then selectively targeted by programmed cell death.

According to this model, programmed cell death would target primarily: (1) the *en*-negative hemilineage of AC and PC neuroblasts; (2) the *en*-positive hemilineage of MC2 neuroblast; and (3) neither hemilineage of the MC1 neuroblast (see Fig. 8). This model makes the following predictions. First, in the AC and PC lineages, most of the surviving neurons should be *en*-positive. Second, in the MC2 lineage, most of the surviving neurons should be *en*-negative. Third, in the MC1 lineage, both *en*-positive and *en*-negative neurons should mostly survive. Fourth, following apoptosis block, all four lineages should be of approximately the same size. Fifth, following apoptosis block, all four lineages should contain comparable numbers of *en*-positive and *en*-negative neurons.

Although the hemilineage model explains the majority of our findings, there are several results that are not in full quantitative accord with it. First, a small number (<5) of *en*-negative neurons are found in AC and PC lineages: the model predicts that all neurons should be *en*-positive. Second, a small number (<10) of *en*-positive neurons are found in the MC2 lineage: the model predicts that all neurons should be *en*-negative. Third, a low level of cell death (involving approximately 20 *en*-negative neurons each) does occur in the MC1 and MC2 lineages: the model predicts that no cell death should occur in the MC1 lineage, and only *en*-positive neurons should die in MC2 lineage.

To test the validity of this model in more detail, we focused on the PC neuroblast lineage and recovered both wild type and H99 single-cell and double-cell MARCM clones, co-immunolabeled with anti-En and anti-Elav. In MARCM experiments, double-cell clones are recovered when both daughter cells of a GMC are labeled following the recombination event, whereas single-cell clones are recovered when only one daughter cell of a GMC is labeled following recombination (see Lee and Luo, 2001). However, a single-cell clone will also be also recovered in place of a double-cell clone if one of the two daughter cells of the GMC undergoes apoptosis between the recombination event and the time of MARCM clone recovery.

According to the model, the *en*-negative hemilineage is primarily targeted by programmed cell death in the wild-type PC lineage. Hence, double-cell clones that comprise both GMC daughter cells should be rare, and single-cell clones should be predominant, in wild-type brains. This was indeed the case (Fig. 6A). In wild type, 87% non-neuroblast clones recovered were single-cell neuronal clones. Also according to the model, following apoptosis block, both *en*-positive and *en*-negative hemilineages survive. Hence, both double-cell clones comprising one *en*-positive and one *en*-negative neuron and single-cell clones should be recovered in apoptosis-blocked clones of the PC lineage. This was also the case (Fig. 6B). Following apoptosis block, double-cell clones and single-cell clones were recovered in approximately equal numbers. Moreover, over 80% of double-cell clones consisted of one *en*-positive and one *en*-negative neuron.

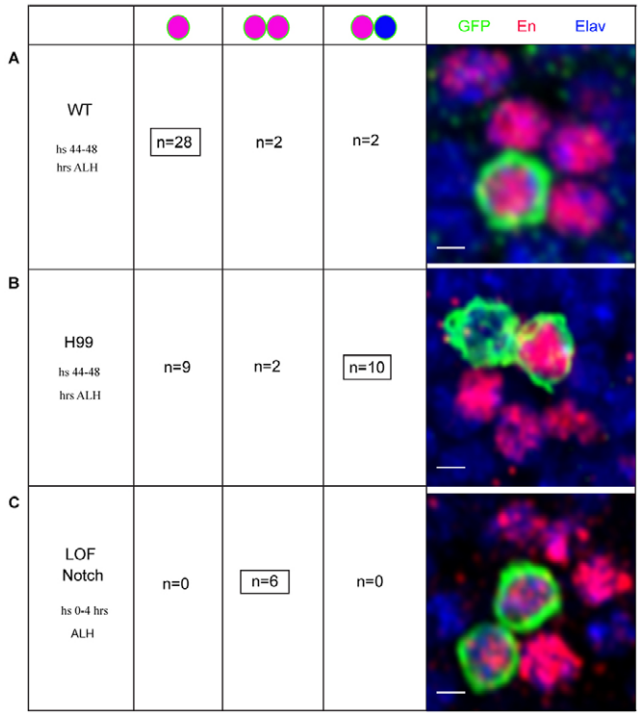

Fig. 6. Evidence for hemilineage-specific cell death in the PC lineage. GFP-labeled single- and two-cell MARCM clones (green) in PC lineage stained with anti-En (red) and anti-Elav (blue). Time of heat-shock treatment is indicated. Top row is a schematic of the clone types examined; pink and blue circles represent *en*-positive and *en*-negative neurons, respectively. *n* shows number of times a clone type was recovered; the most frequent clone type is boxed and represented in the corresponding figure panel. (**A**) Wild-type PC clones. The majority of single *en*-positive neurons (*n*=28 from 286 examined brain hemispheres). Very few two-cell clones were recovered (*n*=4). (**B**) H99 PC clones. The majority are two-cell clones, having an *en*-positive and an *en*-negative neuron (*n*=10 from 280 examined brain hemispheres). Single *en*-positive neurons were also obtained (*n*=9). (**C**) Notch mutant PC MARCM clones. All are two-cell clones with *en*-positive neurons (*n*=6 from 544 examined brain hemispheres). Scale bars: 10 μm.

Finally, as Notch signaling is known to be an important factor in assigning differential cell fate to the two daughter cells of a GMC (see Karcavich, 2005), we blocked Notch signaling in the PC lineage by generating Notch loss-of-function clones. Given that loss of Notch signaling should cause both GMC daughters to adopt the same fate, the model predicts that recovered two-cell clones would consist of two surviving *en*-positive neurons. The experimental results confirm this prediction; all recovered two-cell clones comprised two *en*-positive neurons (Fig. 6C).

Notch signaling influences number of *engrailed*-expressing neurons in a lineage-specific manner

The analysis of Notch mutant two-cell clones in the PC lineage suggests that loss of Notch signaling results in a neuronal-cell-fate transformation such that both daughters of GMCs in this lineage become *en*-positive. To determine if loss of Notch signaling might have comparable effects on *en*-expression in neurons of other *en* lineages, we recovered Notch loss-of-function neuroblast clones for all four lineages. Neuroblast MARCM clones were co-immunolabeled with anti-En and anti-Elav. We then quantified number of *en*-positive and *en*-negative neurons in wild type versus Notch loss-of-function neuroblast clones for each lineage.

In Notch loss-of-function MC1 neuroblast clones, all neurons were *en*-positive; *en*-negative neurons were no longer seen (Fig. 7A,A′). Moreover, as expected, given the low level of programmed cell death in the MC1 lineage, there was no obvious size decrease or increase in mutant versus wild-type clones (see Fig. S1 in the supplementary material). This suggests that most neurons fated to become *en*-negative in wild type adopted an *en*-positive phenotype in the absence of Notch signaling (resulting phenotype schematized in Fig. 7A″).

In Notch loss-of-function AC and PC neuroblast clones, the number of surviving *en*-positive neurons increased markedly (105±9 for AC; 100±7.9 for PC) compared with wild type (63±5.9 for AC; 55±4.7 for PC), whereas the small number (<10) of *en*-negative neurons did not change significantly (Fig. 7B,B″,C,C′). Resulting mutant clones were almost twice as large as wild-type clones (see Fig. S1 in the supplementary material). This is what would be expected if most neurons fated to become *en*-negative in wild type, and thus programmed to die in AC and PC lineages (see Fig. 8), adopted an *en*-positive phenotype and hence survived in the absence of Notch signaling (resulting phenotype schematized in Fig. 7B″,C″).

By contrast, in Notch loss-of-function MC2 neuroblast clones, the number of surviving *en*-negative neurons decreased dramatically (2±2.3) compared with wild type (58±10.8), whereas the small number (<10) of *en*-positive neurons was not affected (Fig. 7D,D′). The resulting mutant clones were very small compared with wild-type clones and did not have a discernable projection pattern, probably due to very few neurons (see Figs S1 and S2 in the supplementary material). This is what would be expected if most neurons fated to become *en*-negative in wild type, and thus programmed to survive in MC2 lineage (see Fig. 8), adopted an *en*-positive phenotype and hence died in the absence of Notch signaling (resulting phenotype schematized in Fig. 7D″).

Taken together, these findings indicate that Notch signaling has lineage-specific effects on the number of *en*-expressing neurons in the four brain neuroblast lineages. Loss of Notch function caused a marked increase in the number of surviving *en*-positive neurons in AC and PC lineages, a dramatic decrease in surviving *en*-negative neurons in the MC2 lineage and an increase in *en*-positive neurons as well as a corresponding decrease in *en*-negative neurons in the MC1 lineage. These results support the hypothesis that loss of Notch

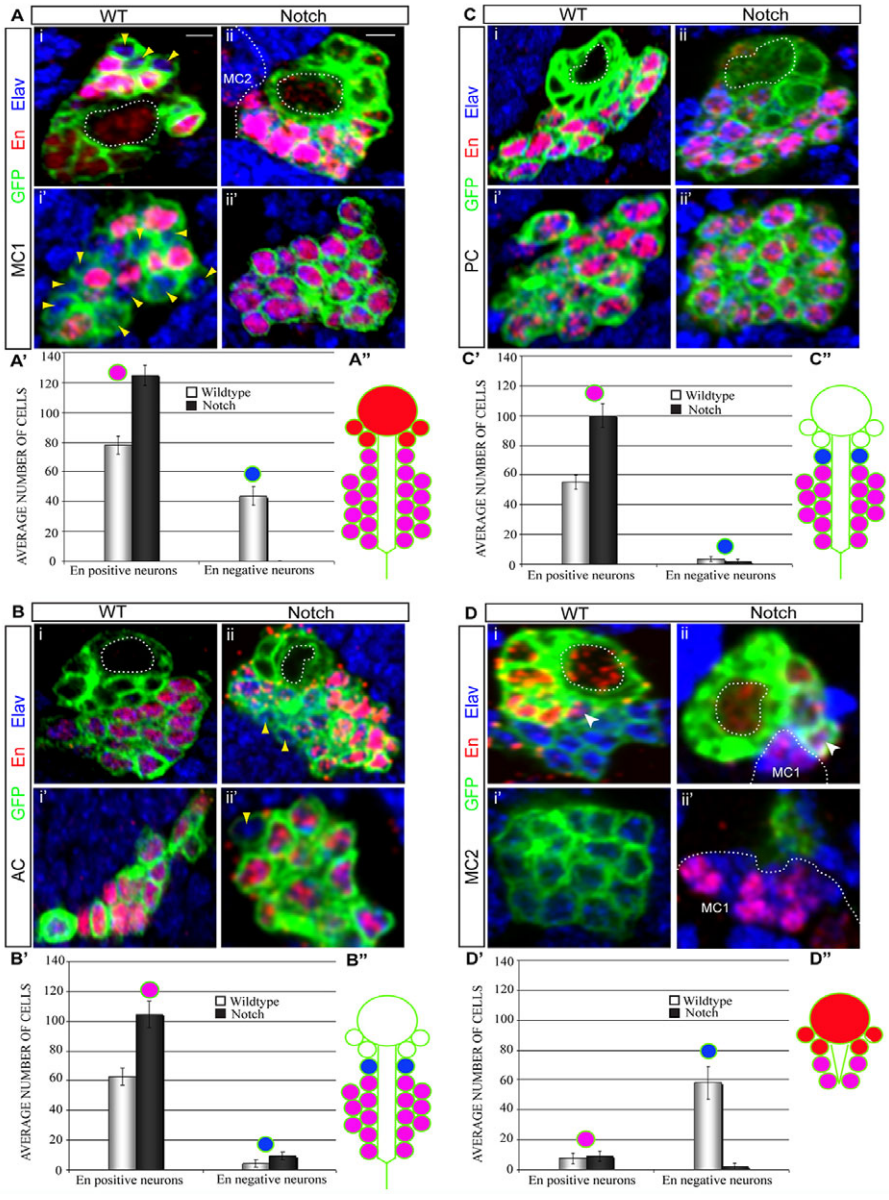

Fig. 7. Effect of loss of Notch function on *engrailed* lineages. (**A-D**) *z*-projections of wild type (i-i′) and Notch mutant (ii-ii′) MARCM clones (MC1, AC, PC and MC2, respectively) stained with anti-GFP (green), anti-En (red) and anti-Elav (blue). The top (i,ii) and bottom (i′,ii′) rows of panels are similar to those of Fig. 5. Yellow arrowheads indicate *en*-negative neurons; white arrowheads indicate *en*-positive neurons. (**A′-D′**) Bar charts showing the effect of loss of Notch function on the number of *en*-positive and *en*-negative neurons, as compared with wild type. (**A″-D″**) Schematics of Notch mutant MC1, AC, PC and MC2 clones, respectively. Color coding is according to immunostaining. Sample size (*n*) for Notch mutant lineages: MC1, *n*=6; AC, *n*=4; PC, *n*=9; and MC2, *n*=7. Error bars indicate s.d. Scale bars: 10 μm.

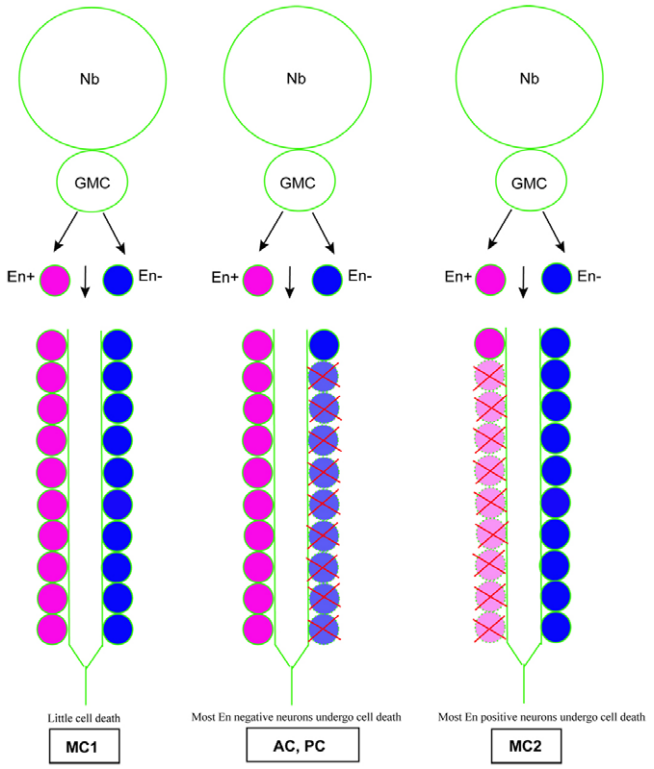

Fig. 8. Model for hemilineage-specific cell death and generation of lineage diversity. The neurons with a dotted border and red cross undergo cell death. En+, *en*-positive neuron; En–, *en*-negative neuron; GMC, ganglion mother cell; Nb, neuroblast.

signaling causes all neurons in the four lineages to acquire an *en*-positive cell fate and the cells to survive or die depending on the lineage-specific context.

DISCUSSION

Lineage-specific cell death in the postembryonic brain

Programmed cell death has been extensively investigated in the embryonic insect CNS. In VNC neuromeres, cell death has an important role in generating dramatic differences in neuronal numbers in abdominal versus thoracic ganglia. Thus, although both abdominal and thoracic neuromeres begin proliferation via a nearly identical number of embryonic neuroblasts, mature thoracic ganglia comprise approximately 3000 neural cells, whereas mature abdominal ganglia comprise approximately 500 neurons. Programmed cell death together with different neuroblast life spans and proliferation rates are responsible for this difference (reviewed by Buss et al., 2006). Segment-specific programmed cell death has also been shown to occur during CNS embryogenesis (Miguel-Aliaga and Thor, 2004; Rogulja-Ortmann et al., 2007).

In postembryonic CNS development of holometabolous insects such as flies, a combination of programmed cell death and neuronal process re-innervation allows the larval nervous system to reorganize and innervate new body structures (Truman, 1983; Truman et al., 1992; Weeks, 2003; Weeks and Truman, 1985). During metamorphosis many adult-specific neurons in the ventral ganglia are targeted by programmed cell death, particularly in abdominal segments (Bello et al., 2003; Booker and Truman, 1987; Booker et al., 1996). Furthermore, extensive cell death occurs during postembryonic development in the insect visual system, where cells are overproduced and those that do not make the appropriate targets are eliminated by apoptosis (Bonini and Fortini, 1999). By contrast, very little is currently known about the prevalence and functional roles of programmed cell death in development of the insect adult central brain.

In this report, we identify four neuroblast lineages in the postembryonic central brain and find that programmed cell death occurs in all four lineages, albeit to different extents. Whereas cell death plays only a minor role in the MC1 lineage, it has dramatic effects in AC, PC and MC2 lineages, in which nearly half of the adult-specific neuronal progeny are programmed to die during larval development. It is noteworthy that the adult-specific neurons targeted by cell death are generated during larval development and are eliminated before their respective neuroblasts stop proliferating (12-24 hours after pupal formation). Because the cell death reported here occurs before neuronal differentiation, it is probably not involved in events of brain reorganization that take place during metamorphosis.

Another central feature of the cell death events demonstrated here is that none of the four lineages is completely eliminated by cell death; all four neuroblasts and a significant number of their neuronal progeny survive at the end of larval development, and these neuronal progeny are largely present in the adult. In this sense, the programmed cell death reported here is likely to be functionally different from the cell death observed in the ventral ganglia, where the neuroblast itself undergoes apoptosis, regulating neuronal numbers in the abdominal segments (Bello et al., 2003; Truman and Bate, 1988).

Our experiments indicate that programmed cell death plays a prominent role in determining lineage-specific features; if cell death is blocked the total neuronal number increases in all four lineages and the number of *en*-expressing neurons increases in AC, PC and MC2. Furthermore, we examined the axonal projection pattern of H99 and Notch mutant *en*-expressing lineages, comparing them to wild type (see Fig. S2 in the supplementary material). Both H99 and Notch mutant PC lineages showed an additional projection that was not present in the wild type, whereas the other three H99 lineages did not appear to change drastically in their projection patterns. In conclusion, programmed cell death appears to contribute to the cellular diversity of neuronal lineages in the central brain.

Differential cell fate, Notch signaling and generation of hemilineages in the brain

Studies on neuroblast lineages in the developing ventral ganglia indicate that proliferating neuroblasts generate a largely invariant clone of neural cells. In general, each neuroblast division produces a distinctly fated GMC, and each GMC division produces two sibling progeny of different fates (reviewed by Technau et al., 2006; Egger et al., 2007). There is some evidence that the fate of these progeny is controlled by the parental GMC; the two siblings are restricted to a pair of different cell fates, with one sibling adopting an ‘A’ fate and the other adopting a ‘B’ fate (J. W. Truman, personal communication) (Skeath and Doe, 1998). This, in turn, has led to a model in which a neuroblast lineage can be thought of as composed of two hemilineages, with one hemilineage comprising ‘A’-fate cells and the other hemilineage comprising ‘B’-fate cells. It is thought that an interaction between Notch and Numb is responsible for generating distinct neural fates of the two GMC daughter cells, with a loss of Notch or Numb resulting in reciprocal cell-fate duplication (Karcavich, and Doe, 2005; Lundell et al., 2003; Novotny et al., 2002). However, Notch signaling does not appear to confer a particular fate; rather, it acts generically as a mechanism to enable two siblings to acquire different fates, and other developmental

control genes that are inherited from the specific parental GMC are thought to be instrumental in determining the final identity of each progeny (Karcavich, 2005).

Our findings on lineage-specific cell death support a comparable model in which all four brain neuroblasts can generate one *en*-positive hemilineage and one *en*-negative hemilineage (Fig. 8). In this model, programmed cell death is then targeted in a lineage-specific manner to either the *en*-negative hemilineage (AC, PC), or the *en*-positive hemilineage (MC2), or neither hemilineage (MC1). Alternatively, *en*-positive and *en*-negative neurons in the lineages could be generated in a temporal fashion and subsequently *en*-positive or *en*-negative neurons could be eliminated in a lineage-specific manner. However, our results suggest that this is unlikely. In particular, in the PC lineage, more than 80% of the two-cell clones examined were composed of one *en*-positive and one *en*-negative cell. If the above did occur, a significant number of two-cell *en*-positive clones should have been obtained along with two-cell clones comprising one *en*-positive and one *en*-negative neuron. Similar analysis of single and two cell clones in the other three *en* lineages is further required to confirm the occurrence of hemilineage-specific programmed cell death.

Based on our experimental results, we postulate that Notch signaling is an important generic mechanism underlying generation of the two different hemilineages, as in the absence of Notch signaling, cell-fate duplication of GMC siblings occurs (Fig. 6). Indeed, our analysis of Notch loss-of-function neuroblast clones suggests that in the absence of Notch signaling most of the neurons in the four lineages acquire an *en*-positive cell fate (Fig. 7). Alternatively, in the four lineages examined, being positive for *en* may be the default state of the cells, and Notch induces secondary fate by repressing *en* in subsets of cells in each lineage. These *en*-positive neurons then appear to survive or undergo programmed cell death depending on the lineage-specific context. However, it remains to be seen whether Notch itself acts on the apoptotic machinery, independent of *en*.

In this study, we used *en* as a molecular marker to identify four lineages in the postembryonic central brain. Might *en* itself be functionally involved in regulating programmed cell death in these lineages? For the PC lineage, there is some indication that the total clone size is reduced by approximately half in *en* loss-of-function mutants, compared with wild type (A.K., unpublished). Although this suggests that *en* may be involved in promoting survival of *en*-positive neurons in PC (and probably AC), it does not explain the role of *en* in the MC2 lineage, where it would have to play an opposing role, as *en*-positive neurons die in this lineage. Thus, *en* could act either as a pro-apoptotic or an anti-apoptotic factor, depending on the lineage-specific context. Moreover, a direct genetic interaction between *en* and the apoptotic machinery remains to be investigated. As *en* is known to have multiple interactions with other proteins (Alexandre and Vincent, 2003; Chanas and Maschat, 2005; Joly et al., 2007; Kobayashi et al., 2003), a complex regulatory network involving target proteins of *en* may be responsible for regulating apoptosis in a lineage-specific manner. Further analysis of interactions with such target proteins is necessary to reveal the full regulatory network in more detail.

Serial homology of brain neuroblast lineages?

The lineage-specific effects of cell death and of Notch signaling in AC and PC are distinctly different from those observed in MC1 or MC2 lineages. However, when compared with each other, many aspects of AC and PC lineages are similar. In wild type, both lineages consist of similar numbers of adult-specific neurons, and the majority (approximately 80%) of these neurons are positive for *en*, whereas neuroblasts and GMCs are negative for *en* in both lineages. Blocking cell death results in a substantial (approximately double) increase in total cell number in both lineages, and this increase is almost exclusively due to an increase in the number of surviving *en*-negative neurons in both lineages. Moreover, loss of Notch function causes a marked increase in the number of surviving *en*-positive neurons without affecting the number of *en*-negative neurons in both lineages. The only significant difference between AC and PC lineages observed in this study is that the AC lineage is located in the protocerebrum, whereas the PC lineage is located in the deutocerebrum (Kumar et al., 2009).

What might be responsible for these similarities in the AC and PC neuroblast lineages? There is some evidence for the existence of serially homologous neuroblasts in the fly brain and VNC (Urbach and Technau, 2003b). In the VNC, serially homologous neuroblasts, defined by comparable time of formation, similar positions in the neuromeric progenitor array and similar expression of developmental control genes, such as segment polarity genes, dorsoventral patterning genes and other molecular markers, can give rise to almost identical cell lineages (Bhat, 1999; Bossing et al., 1996; Broadus and Doe, 1995; Doe, 1992; Schmidt et al., 1997). This suggests that similar regulatory interactions take place during development of serially homologous neuroblasts and their neural lineages. A comparison of molecular expression patterns in neuroblasts from different neuromeres of the brain and ventral ganglia suggests that several of them might be serial homologs of each other (Urbach and Technau, 2003b). For example, neuroblasts NB5-6 in the abdominal, thoracic and subesophageal ganglia have been proposed to be homologous to NBDd7 in the deutocerebrum and NBTd4 in the tritocerebrum.

Given the remarkable similarities in AC and PC neuroblast lineages, it is possible that the protocerebral AC lineage and the deutocerebral PC lineages represent serial homologs. If this is the case, then investigations of the cellular and molecular mechanisms that control their lineage-specific development should be useful for our understanding of how regionalized neural diversity in the brain evolves from a basic metameric ground state. However, as neither the combination of developmental control genes expressed in AC and PC neuroblasts nor the position of the two brain neuroblasts in their neuromeres of origin are currently known in sufficient detail, further experiments are needed before the issue of serial homology can be resolved for these brain neuroblast lineages.

Acknowledgements

We thank Dr Robert Lichtneckert for discussions and Susanne Flister for technical help. This study was funded by Swiss NSF Grant 3100A0-112024 to H.R.

Supplementary material

Supplementary material for this article is available at
http://dev.biologists.org/cgi/content/full/136/20/3433/DC1

References

Abrams, J. M., White, K., Fessler, L. I. and Steller, H. (1993). Programmed cell death during Drosophila embryogenesis. *Development* **117**, 29-43.

Alexandre, C. and Vincent, J. P. (2003). Requirements for transcriptional repression and activation by Engrailed in Drosophila embryos. *Development* **130**, 729-739.

Awad, T. A. and Truman, J. W. (1997). Postembryonic development of the midline glia in the CNS of Drosophila: proliferation, programmed cell death, and endocrine regulation. *Dev. Biol.* **187**, 283-297.

Bello, B. C., Hirth, F. and Gould, A. P. (2003). A pulse of the Drosophila Hox protein Abdominal-A schedules the end of neural proliferation via neuroblast apoptosis. *Neuron* **37**, 209-219.

Bello, B. C., Holbro, N. and Reichert, H. (2007). Polycomb group of genes are required for neural stem cell survival in postembryonic neurogenesis of Drosophila. *Development* **134**, 1091-1099.

Bello, B. C., Izergina, N., Caussinus, E. and Reichert, H. (2008). Amplification of neural stem cell proliferation by intermediate progenitor cells in Drosophila brain development. *Neural Dev.* **3**, 5.
Bhat, K. M. (1999). Segment polarity genes in neuroblast formation and identity specification during Drosophila neurogenesis. *BioEssays* **21**, 472-485.
Bonini, N. M. and Fortini, M. E. (1999). Surviving Drosophila eye development: integrating cell death with differentiation during formation of a neural structure. *BioEssays* **21**, 991-1003.
Booker, R. and Truman, J. W. (1987). Postembryonic neurogenesis in the CNS of the tobacco hornworm, Manduca sexta. I. Neuroblast arrays and the fate of their progeny during metamorphosis. *J. Comp. Neurol.* **255**, 548-559.
Booker, R., Babashak, J. and Kim, J. B. (1996). Postembryonic neurogenesis in the central nervous system of the tobacco hornworm, Manduca sexta. III. Spatial and temporal patterns of proliferation. *J. Neurobiol.* **29**, 233-248.
Boone, J. Q. and Doe, C. Q. (2008). Identification of Drosophila type II neuroblast lineages containing transit amplifying ganglion mother cells. *Dev. Neurobiol.* **68**, 1185-1195.
Bossing, T., Udolph, G., Doe, C. Q. and Technau, G. M. (1996). The embryonic central nervous system lineages of Drosophila melanogaster. I. Neuroblast lineages derived from the ventral half of the neuroectoderm. *Dev. Biol.* **179**, 41-64.
Bowman, S. K., Rolland, V., Betschinger, J., Kinsey, K. A., Emery, G. and Knoblich, J. A. (2008). The tumor suppressors Brat and Numb regulate transit-amplifying neuroblast lineages in Drosophila. *Dev. Cell* **14**, 535-546.
Broadus, J. and Doe, C. Q. (1995). Evolution of neuroblast identity: seven-up and prospero expression reveal homologous and divergent neuroblast fates in Drosophila and Schistocerca. *Development* **121**, 3989-3996.
Buss, R. R., Sun, W. and Oppenheim, R. W. (2006). Adaptive roles of programmed cell death during nervous system development. *Annu. Rev. Neurosci.* **29**, 1-35.
Cayouette, M. and Raff, M. (2002). Asymmetric segregation of Numb: a mechanism for neural specification from Drosophila to mammals. *Nat. Neurosci.* **5**, 1265-1269.
Chanas, G. and Maschat, F. (2005). Tissue specificity of hedgehog repression by the Polycomb group during Drosophila melanogaster development. *Mech. Dev.* **122**, 975-987.
Chen, P., Nordstrom, W., Gish, B. and Abrams, J. (1996). grim, a novel cell death gene in Drosophila. *Genes Dev.* **10**, 1773-1782.
Doe, C. Q. (1992). Molecular markers for identified neuroblasts and ganglion mother cells in the Drosophila central nervous system. *Development* **116**, 855-863.
Dumstrei, K., Wang, F., Nassif, C. and Hartenstein, V. (2003). Early development of the Drosophila brain: V. Pattern of postembryonic neuronal lineages expressing DE-cadherin. *J. Comp. Neurol.* **455**, 451-462.
Egger, B., Boone, J. Q., Stevens, N. R., Brand, A. H. and Doe, C. Q. (2007). Regulation of spindle orientation and neural stem cell fate in the Drosophila optic lobe. *Neural Dev.* **2**, 1.
Grether, M., Abrams, J., Agapite, J., White, K. and Steller, H. (1995). The head involution defective gene of Drosophila melanogaster functions in programmed cell death. *Genes Dev.* **9**, 1694-1708.
Hidalgo, A. and Constant, f.-C. (2003). The control of cell number during central nervous system development in flies and mice. *Mech. Dev.* **120**, 1311-1325.
Huang, F. D., Matthies, H. J., Speese, S. D., Smith, M. A. and Broadie, K. (2004). Rolling blackout, a newly identified PIP2-DAG pathway lipase required for Drosophila phototransduction. *Nat. Neurosci.* **7**, 1070-1078.
Joly, W., Mugat, B. and Maschat, F. (2007). Engrailed controls the organization of the ventral nerve cord through frazzled regulation. *Dev. Biol.* **301**, 542-554.
Karcavich, R. E. (2005). Generating neuronal diversity in the Drosophila central nervous system: a view from the ganglion mother cells. *Dev. Dyn.* **232**, 609-616.
Karcavich, R. and Doe, C. Q. (2005). Drosophila neuroblast 7-3 cell lineage: a model system for studying programmed cell death, Notch/Numb signaling, and sequential specification of ganglion mother cell identity. *J. Comp. Neurol.* **481**, 240-251.
Knoblich, J. A. (2008). Mechanisms of asymmetric stem cell division. *Cell* **132**, 583-597.
Kobayashi, M., Fujioka, M., Tolkunova, E. N., Deka, D., Abu-Shaar, M., Mann, R. S. and Jaynes, J. B. (2003). Engrailed cooperates with extradenticle and homothorax to repress target genes in Drosophila. *Development* **130**, 741-751.
Kumar, A., Fung, S., Lichtneckert, R., Reichert, H. and Hartenstein, V. H. (2009). Arborization pattern of engrailed-expressing neural lineages reveal neuromere boundaries in the Drosophila brain neuropile. *J. Comp. Neurol.* **517**, 87-104.
Lee, T. and Luo, L. (1999). Mosaic analysis with a repressible cell marker for studies of gene function in neuronal morphogenesis. *Neuron* **22**, 451-461.
Lee, T. and Luo, L. (2001). Mosaic analysis with a repressible cell marker (MARCM) for Drosophila neural development. *Trends Neurosci.* **24**, 251-254.
Lu, B., Jan, L. and Jan, Y. N. (2000). Control of cell divisions in the nervous system: symmetry and asymmetry. *Annu. Rev. Neurosci.* **23**, 531-556.
Lundell, M. J., Lee, H. K., Perez, E. and Chadwell, L. (2003). The regulation of apoptosis by Numb/Notch signaling in the serotonin lineage of Drosophila. *Development* **130**, 4109-4121.
Miguel-Aliaga, I. and Thor, S. (2004). Segment-specific prevention of pioneer neuron apoptosis by cell-autonomous, postmitotic Hox gene activity. *Development* **131**, 6093-6105.
Novotny, T., Eiselt, R. and Urban, J. (2002). Hunchback is required for the specification of the early sublineage of neuroblast 7-3 in the Drosophila central nervous system. *Development* **129**, 1027-1036.
Orgogozo, V., Schweisguth, F. and Bellaiche, Y. (2002). Binary cell death decision regulated by unequal partitioning of Numb at mitosis. *Development* **129**, 4677-4684.
Pearson, B. J. and Doe, C. Q. (2004). Specification of temporal identity in the developing nervous system. *Annu. Rev. Cell Dev. Biol.* **20**, 619-647.
Pereanu, W. and Hartenstein, V. (2006). Neural lineages of the Drosophila brain: a three-dimensional digital atlas of the pattern of lineage location and projection at the late larval stage. *J. Neurosci.* **26**, 5534-5553.
Peterson, C., Carney, G. E., Taylor, B. J. and White, K. (2002). *reaper* is required for neuroblast apoptosis during Drosophila development. *Development* **129**, 1467-1476.
Prokop, A. and Technau, G. M. (1991). The origin of postembryonic neuroblasts in the ventral nerve cord of Drosophila melanogaster. *Development* **111**, 79-88.
Rogulja-Ortmann, A., Luer, K., Seibert, J., Rickert, C. and Technau, G. M. (2007). Programmed cell death in the embryonic central nervous system of Drosophila melanogaster. *Development* **134**, 105-116.
Rogulja-Ortmann, A., Renner, S. and Technau, G. M. (2008). Antagonistic roles for *Ultrabithorax* and *Antennapedia* in regulating segment-specific apoptosis of differentiated motoneurons in the Drosophila embryonic central nervous system. *Development* **135**, 3435-3445.
Schmid, A, Chiba, A. and Doe, C. Q. (1999). Clonal analysis of Drosophila embryonic neuroblasts: neural cell types, axon projections and muscle targets. *Development* **126**, 4653-4689.
Schmidt, H., Rickert, C., Bossing, T., Vef, O., Urban, J. and Technau, G. M. (1997). The embryonic central nervous system lineages of Drosophila melanogaster. II. Neuroblast lineages derived from the dorsal part of the neuroectoderm. *Dev. Biol.* **189**, 186-204.
Skeath, J. B. and Doe, C. Q. (1998). Sanpodo and Notch act in opposition to Numb to distinguish sibling neuron fates in the Drosophila CNS. *Development* **125**, 1857-1865.
Skeath, J. B. and Thor, S. (2003). Genetic control of Drosophila nerve cord development. *Curr. Opin. Neurobiol.* **13**, 8-15.
Sonnenfeld, M. J. and Jacobs, J. R. (1995). Apoptosis of the midline glia during Drosophila embryogenesis: a correlation with axon contact. *Development* **121**, 569-578.
Technau, G. M., Berger, C. and Urbach, R. (2006). Generation of cell diversity and segmental pattern in the embryonic central nervous system of Drosophila. *Dev. Dyn.* **235**, 861-869.
Truman, J. W. (1983). Programmed cell death in the nervous system of an adult insect. *J. Comp. Neurol.* **212**, 445-452.
Truman, J. W. and Bate, M. (1988). Spatial and temporal patterns of neurogenesis in the central nervous system of Drosophila melanogaster. *Dev. Biol.* **125**, 145-157.
Truman, J. W., Thorn, R. S. and Robinow, S. (1992). Programmed neuronal death in insect development. *J. Neurobiol.* **23**, 1295-1311.
Truman, J. W., Schuppe, H., Shepherd, D. and Williams, D. W. (2004). Developmental architecture of adult-specific lineages in the ventral CNS of Drosophila. *Development* **131**, 5167-5184.
Urbach, R. and Technau, G. M. (2003a). Segment polarity and DV patterning gene expression reveals segmental organization of the Drosophila brain. *Development* **130**, 3607-3620.
Urbach, R. and Technau, G. M. (2003b). Molecular markers for identified neuroblasts in the developing brain of Drosophila. *Development* **130**, 3621-3637.
Urbach, R. and Technau, G. M. (2003c). Early steps in building the insect brain: neuroblast formation and segmental patterning in the developing brain of different insect species. *Arthropod. Struct. Dev.* **32**, 103-123.
Weeks, J. C. (2003). Thinking globally, acting locally: steroid hormone regulation of the dendritic architecture, synaptic connectivity and death of an individual neuron. *Prog. Neurobiol.* **70**, 421-442.
Weeks, J. C. and Truman, J. W. (1985). Independent steroid control of the fates of motoneurons and their muscles during insect metamorphosis. *J. Neurosci.* **5**, 2290-2300.
White, K., Grether, M. E., Abrams, J. M., Young, L., Farrell, K. and Steller, H. (1994). Genetic control of programmed cell death in Drosophila. *Science* **264**, 677-683.
Younossi-Hartenstein, A., Nassif, C., Green, P. and Hartenstein, V. (1996). Early neurogenesis of the Drosophila brain. *J. Comp. Neurol.* **370**, 313-329.
Zheng, X., Zugates, C. T., Lu, Z., Shi, L., Bai, J. M. and Lee, T. (2006). Baboon/dSmad2 TGF-beta signaling is required during late larval stage for development of adult-specific neurons. *EMBO J.* **25**, 615-627.